

# Poling of soft piezoceramic PZT

T.M. Kamel, F.X.N.M. Kools, G. de With\*

Laboratory of Materials and Interface Chemistry, Eindhoven University of Technology, 5600 MB Eindhoven, the Netherlands

Received 10 May 2006; received in revised form 24 August 2006; accepted 30 August 2006

Available online 9 October 2006

## Abstract

The properties of piezoelectric ceramic materials are strongly dependent on the degree of polarization as set by the poling process. In the present work a soft piezoceramic PZT material was polarized at different poling conditions. The hysteresis loop, the polarization current and pyroelectric current measurements were used to evaluate the polarization state of the material. The hysteresis loop was monitored using a home-made computer controlled Sawyer–Tower circuit. The polarization current was recorded during the poling process at different applied electric fields, poling time and temperature. The pyroelectric coefficient and the polarization were calculated from the pyroelectric current. The polarization calculated from these data was in excellent agreement with the polarization as calculated from the poling current. The relative permittivity and loss factor were measured as a function of temperature after different poling conditions. The effects of the various poling conditions on the dielectric and ferroelectric properties of the soft PZT are discussed. It is shown that, contrary to common practice, poling at a field slightly larger than the coercive field is adequate to reach full polarization at room temperature.

© 2006 Elsevier Ltd. All rights reserved.

**Keywords:** Piezoelectric; Ferroelectric; Dielectric; PZT; Polarization

## 1. Introduction

Over decades, great attention has been paid to  $[\text{PbTi}_x\text{Zr}_{1-x}\text{O}_3]$  solid solutions for their extremely strong piezoelectric effect.<sup>1–4</sup> The coupling factor and relative permittivity are the highest near the morphotropic phase boundary<sup>1,2,4</sup> making these materials extensively used in actuator devices and microelectromechanical systems (MEMS).<sup>1–3</sup> Poling conditions required to achieve the optimal piezoelectric characteristics widely vary for different materials.<sup>1</sup> Generally, the major objective in all poling stages is to induce the maximum degree of domain alignment by using the lowest electric field, at a temperature as close as possible to room temperature (RT) and in the shortest possible time.

Although the poling of piezoceramics after manufacturing is a crucial process and the effect of poling conditions on the piezoelectric properties has been studied by many authors,<sup>5–9</sup> there is not yet a solid model or theory that governs the poling mechanism for a wide spectrum of piezoelectric materials. In the present paper, we give preliminary results for studying the effect

of the poling conditions on the polarization state as well as on the dielectric and ferroelectric properties. The polarization state has been evaluated by different techniques via which an attempt has been made to explain the poling process.

## 2. Theory

### 2.1. Dielectric response

The most obvious physical reason for time-dependent dielectric response is the inevitable “inertia” of polarization processes.<sup>10</sup> By contrast to a dielectric material system the response of free space is instantaneous and therefore the induced charge ( $\epsilon_0 E$ ) arising from the response of free space follows the field instantaneously. Thus, the charges induced at the sample electrodes will be given by the sum of an instantaneous free space contribution and the delayed material polarization

$$D(t) = \epsilon_0 E + P(t) \quad (1)$$

Here  $D(t)$  denotes dielectric displacement and it represents the total charge density induced at the electrodes. Assuming that a homogeneous electric field  $E$  is applied to a dielectric material, the current density  $J(t)$  through the surface of the material is

\* Corresponding author. Tel.: +31 40 247 4947; fax: +31 40 244 5619.  
E-mail address: [G.d.With@tue.nl](mailto:G.d.With@tue.nl) (G. de With).

the sum of the displacement current  $dD/dt$  and the conduction current  $E/\rho$  and can be written as:

$$J(t) = \frac{dD(t)}{dt} + \frac{E}{\rho} \quad (2)$$

where  $\rho$  is the dc electrical resistivity. Substituting Eq. (1) in Eq. (2) and taking into account that  $E$  is constant during poling, leads to:

$$J(t) = \frac{dP(t)}{dt} + \frac{E}{\rho} \quad (3)$$

The polarization current  $dP/dt$  arises from the tendency of the polarizing species in the material to respond in a delayed manner to the exciting field and must go to zero at infinitely long time. In this sense, this current characterizes the most important property of the dielectric system. On the other hand, the conduction current  $E/\rho$  is constant with time and arises from a continuous movement of free charges across the dielectric material from one electrode to another and this current does not change in any way the “centre of gravity” of the charge distribution in the system.

## 2.2. Polarization switching

Grains in ferroelectric ceramics and polycrystalline films contain always multiple domains. Each domain has its own polarization direction. If the polarization directions through the material are random or distributed in such a way that it leads to a zero net polarization, the pyroelectric and piezoelectric effects of individual domains will cancel and such material is neither pyroelectric nor piezoelectric.

Polycrystalline ferroelectric materials can be brought into a polar state by applying an adequate electric field. This process, which is referred to as poling, can reorient domains within individual grains in the direction of the field. A poled polycrystalline ferroelectric exhibits pyroelectric and piezoelectric properties, even if many domain walls are still present.

By definition, *poling* is the dipole alignment by the electric field. The polarization after the removal of the field (at zero field) is called *remanent polarization*,  $P_r$ . The field necessary to bring the polarization to zero is called the *coercive field*,  $E_C$ .<sup>11</sup> The *spontaneous polarization*  $P_s$  can be defined as the surface charge density<sup>16,31</sup> or the dielectric displacement of polar material when  $\epsilon_r \gg 1$ ,<sup>2</sup> or the dipole moment per unit volume.<sup>20,21</sup> It should be noted that the coercive field  $E_C$  that is determined from the intercept of the hysteresis loop with the field axis is *not* an absolute threshold field.<sup>12</sup> If a low electric field is applied opposite to the polarization over a long time, the polarization will eventually switch to the opposite direction.<sup>11,12</sup> The mechanism of polarization switching has been studied in detail for many bulk and thin-film ferroelectrics.<sup>12–16</sup> However, the issue is not yet well generalized and there is no universal mechanism valid for polarization reversal in all ferroelectrics.

The switching in ferroelectrics takes place by nucleation of domains, characterized by “the nucleation time,  $t_n$ ”, the time necessary to form all nuclei and domain wall motion, characterized by “the domain wall motion time,  $t_d$ ”, the time necessary for one domain to move through the sample. As proposed by

Merz<sup>13</sup> and Merz and Fatuzzo<sup>14</sup> the total switching time can then be approximated by

$$t_s \approx t_n + t_d = t_n + \frac{d}{\mu E} \quad (4)$$

where  $d$  is the distance that the wall travels and  $\mu$  is the mobility of the domain wall. In Merz’s model, it was assumed that the nucleation of new domains is governed by a statistical law, in which at *low fields*, the probability of forming new domains  $p_n$  depends exponentially on the applied field in the following way:

$$p_n = p_0 e^{-\alpha/E}$$

and, since  $t_n \sim 1/p_n$ ,

$$t_n = t_0 e^{\alpha/E} \quad (5)$$

Then, the maximum switching current may be described by

$$J_{\max} = J_{\infty} e^{-\alpha/E}, \quad \text{where } J_{\infty} = (J_{\max})_{E=\infty} \quad (6)$$

Parameters  $\alpha$ ,  $p_0$ ,  $t_0$  and  $J_{\infty}$  are temperature dependent, with switching time decreasing as the Curie point is approached.<sup>11,13–15,17,18</sup> The parameter  $\alpha$  is called the activation field, and can be considered as the threshold of the field needed to initiate nucleation.<sup>15</sup> In the low-field range, the experimental curve can be described by Eq. (5) only while in the high field Eq. (4) is required. Since  $t_s = t_n + t_d$ , one can conclude that the switching time  $t_s$  is determined by the slower of the two mechanisms (nucleation or domain wall motion). At low fields the rate of nucleation is low so that the switching is primarily governed by the nucleation ( $t_n \gg t_d$ ) leading to an exponential law for the switching time. On the other hand, we assume that at high fields the rate of nucleation is extremely large so that the switching time is primarily determined by the velocity of the domain walls ( $t_d \gg t_n$ ).

The field applied antiparallel to the polarization switches the polarization from state  $-P$  to  $+P$ . In his experiment, Merz showed that the total polarization current curve consists of two parts.<sup>12,13</sup> The first part is due to the fast linear response of the dielectric and the second part is the current due to polarization switching. The total area under the curve is equal to

$$\int_0^{t_s} J(t) dt = \epsilon_0 E + 2P \quad (7)$$

Although Merz’s theory was developed for single crystals, it has been applied to polycrystalline materials as well (e.g., ref. 18).

## 3. Experimental techniques

Non-poled polycrystalline ceramic samples of soft PZT (PXE52, donor doped  $\text{PbZr}_{0.415}\text{Ti}_{0.585}\text{O}_3$ ) were obtained from Morgan Electro Ceramics BV, Eindhoven, the Netherlands. The dimensions of the samples under study were 5 mm  $\times$  5 mm  $\times$  0.2 mm.

The first step in examining the poling effect was to reveal the domain structure. The microstructure of poled as well as non-poled samples was investigated using scanning electron

microscopy (JEOL, JSM 840A, Japan). First, the sample was molded in conductive resin, ground and successively polished. Then the sample surface was etched using 95% water, 5% HCl, five to six drops of HF as an etching agent.<sup>19</sup> Next, the sample surfaces were coated with gold by sputtering. The cross-section normal to the polarization direction was investigated.

The measurements of polarization can be directly made by reversing the spontaneous polarization with the applied electric field. A computer controlled Sawyer–Tower circuit was used to examine the ferroelectric hysteresis loop. The remanent polarization  $P_r$  and coercive field  $E_C$  were measured as a function of temperature.

The polarization current measurements were carried out using a Keithley 6517 Electrometer on initially non-poled samples, provided with Ni-sputtered electrodes covering the complete surface, at different applied electric fields and temperatures. The electric field was applied using the Keithley built-in voltage source and varied from 2.5 to 25 kV/cm with a response time of 5 ms (100 V) and 80 ms (1000 V). For high-temperature measurements, a set-up in a “Linn Elektronika” oven was used. The temperature was measured using a type-K thermocouple. The poling current was continuously recorded while the sample temperature was kept at a fixed value. The polarization was then calculated by integrating the experimental poling current density  $J_{pol}$  over the whole measuring time  $t$ .<sup>10</sup>

$$P = \int_0^t J_{pol} dt \quad (8)$$

After the poling process, the sample was short-circuited.

The pyroelectric measurements were carried out using the direct method.<sup>20</sup> Using this method a sample poled at least a day in advance was situated in an oven heated at a constant heating rate  $dT/dt$  of 0.058 °C/s. The two electrodes were short-circuited via Keithley 6517 electrometer to measure the pyroelectric electric current. The pyroelectric coefficient  $p$  was calculated in terms of the pyroelectric current  $I_{pyro}$  by

$$p = \frac{I_{pyro}}{A} \left( \frac{dT}{dt} \right)^{-1} \quad (9)$$

where  $A$  is the electrode area. The spontaneous polarization  $P_s$  was calculated by integrating the pyroelectric coefficient

$$P_s = - \int p dT \quad (10)$$

The dielectric parameters ( $\epsilon_r$ ,  $\tan \delta$ ) of poled and non-poled samples were measured using RCL Bridge (4284A Precision LCR Meter) at 1 kHz in the temperature range from room temperature up to 250 °C.

## 4. Results

### 4.1. Microstructure

Fig. 1 shows the SEM micrographs of a poled sample. The alignment of the domains is clearly revealed after the application of the applied electric field (15 kV/cm). The average

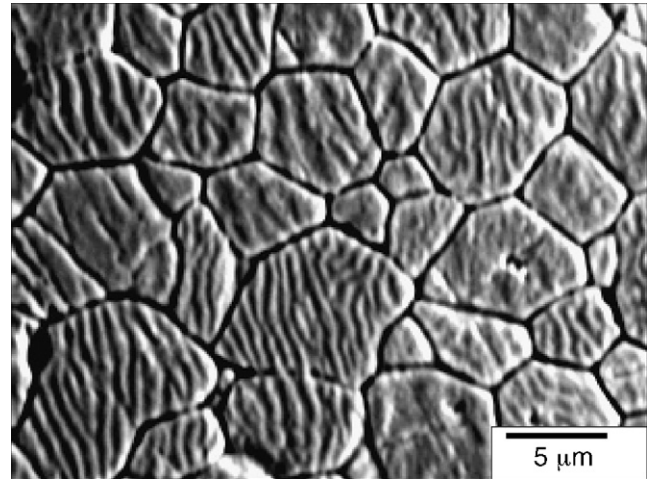


Fig. 1. SEM micrograph of a poled sample. The applied field was (15 kV/cm).

grain size is 4.5 μm as determined by the linear intercept method.

### 4.2. Hysteresis loop

The hysteresis loop was observed at 1 Hz to get the highest polarization. At room temperature the hysteresis loop showed that the saturation polarization  $P_{sat}$  is 42.5 μC/cm<sup>2</sup>, the remanent polarization  $P_r$  is 35.7 μC/cm<sup>2</sup> and the coercive field  $E_C$  is 7.5 kV/cm. Both  $P_r$  and  $E_C$  were measured as a function of temperature (Fig. 2) and are typically decreasing with temperature, rapidly approaching (nearly) zero at 170 °C. This temperature is referred to as the Curie temperature  $T_C$ .

Worthwhile to mention is that  $P_r$  still survives even above  $T_C$  which means that the material shows *relaxor-like* behavior.<sup>11,21–24</sup> Also the hysteresis loop was traced with temperature (Fig. 3). As the temperature increases the loop collapses and becomes slimmer with vanishing  $P_r$  and  $E_C$  but still surviving even above  $T_C$ .

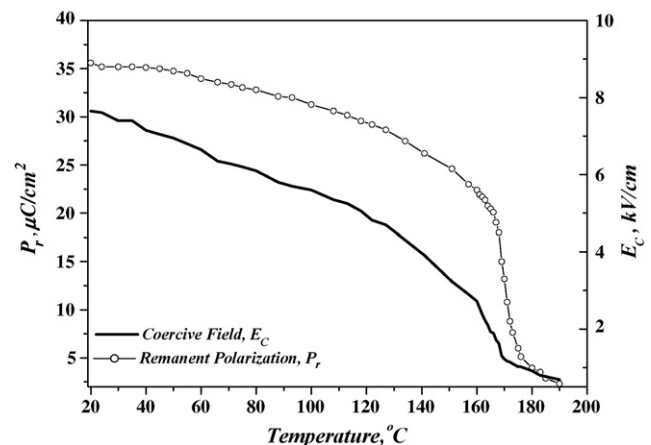


Fig. 2. Remanent polarization ( $P_r$ ) and coercive field ( $E_C$ ) as a function of temperature. The applied frequency is 1 Hz.

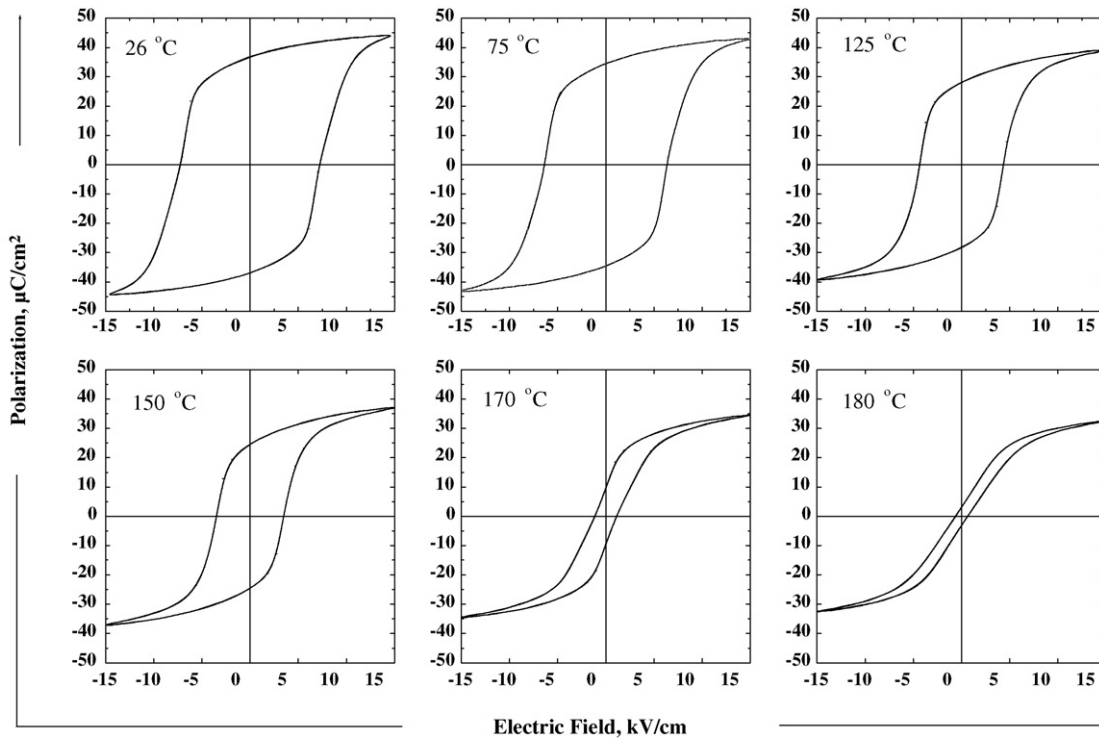


Fig. 3. Hysteresis loop as a function of temperature. The polarization reversal with small  $E_C$  and  $P_r$  is still persistent after  $T_C = 170^\circ\text{C}$ . Applied frequency 5 Hz.

4.3. Polarization current

The polarization current as a function of time at different low fields ( $E < E_C$ ) (2.5–6 kV/cm) was measured at room temperature (Fig. 4). The polarization current is initially high and then shows a fast decay with time passing a hump at a certain time for certain field. The hump is moving towards shorter time as the applied field is increasing until it completely diffuses within the initial high pulse when the coercive field is approached. No steady-state current is observed in this range of electric field meaning that the material is still being polarized.

Worthwhile to mention is that at very low field no humps were observed in the time interval used. Apparently, it needed a longer time than  $3 \times 10^3$  s. It was, however, found that by increasing

the sample temperature, the hump appeared at reasonable time and moved towards shorter time as the temperature increases at a rate dependant on the field applied (Figs. 5 and 6). For higher fields ( $E \geq E_C$ ), the shape of poling current curves looks very different. As the initial current is inversely proportional to the applied electric field (contrary to a low-field case), a steady-state current, directly proportional to the applied field, appeared after a relatively long time (Fig. 7).

4.4. Pyroelectric current

The pyroelectric coefficient was calculated using Eq. (9) (Fig. 8) and shows a very sharp peak at  $168^\circ\text{C}$  which is associ-

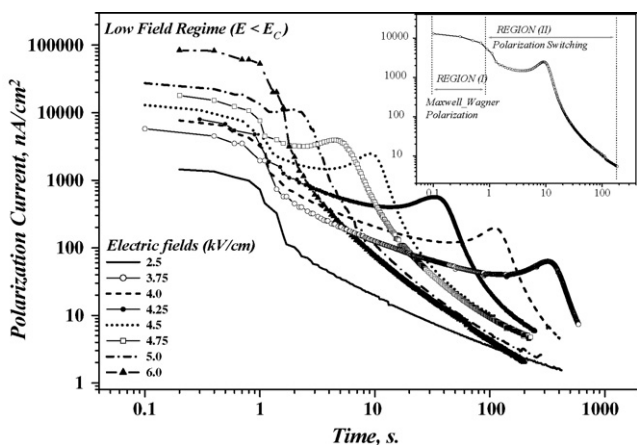


Fig. 4. Polarization current as a function of time at different applied poling fields ( $E < E_C$ ). For each curve a different non-poled sample was taken.

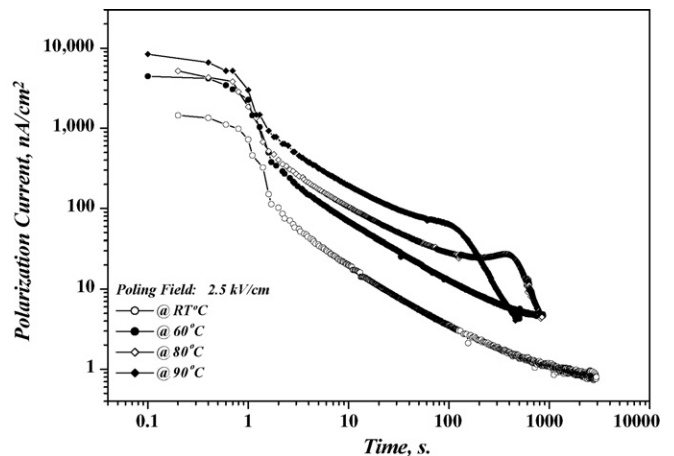


Fig. 5. Polarization current as a function of time at 2.5 kV/cm at different temperatures.



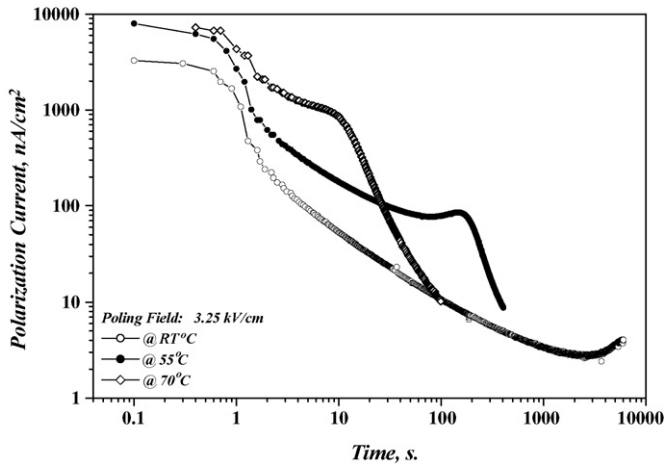


Fig. 6. Polarization current as a function of time at 3.25 kV/cm at different temperatures.

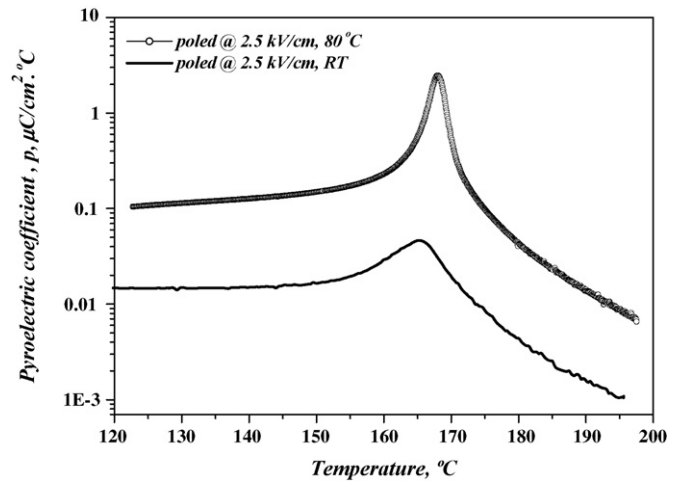


Fig. 9. Pyroelectric coefficient of the two samples poled at 2.5 kV/cm at room temperature and 80 °C, respectively.

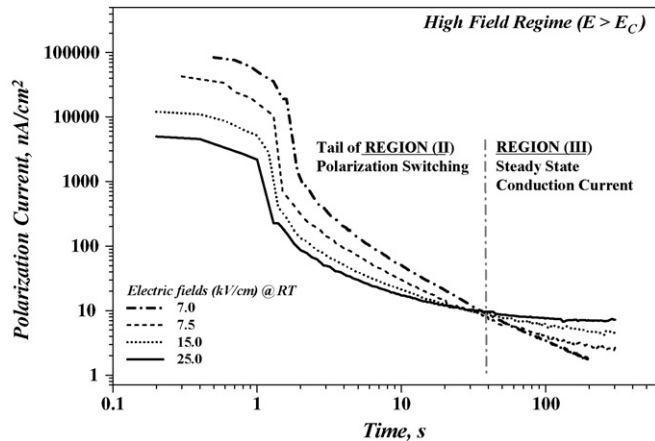


Fig. 7. Polarization current as a function of time at different applied poling fields ( $E > E_C$ ). For each curve a different non-poled sample was taken.

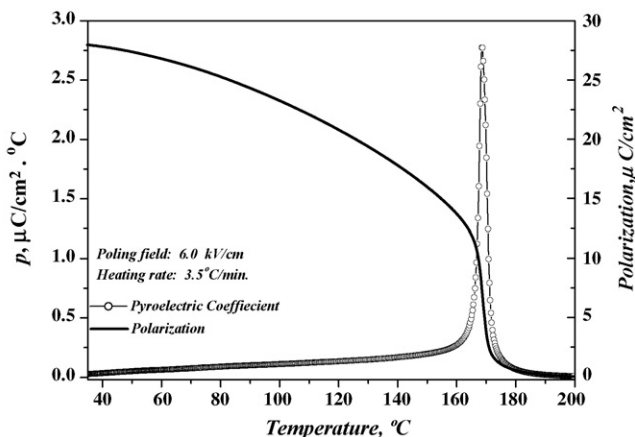


Fig. 8. The pyroelectric coefficient and the calculated polarization for a prepoled sample.

ated with the ferroelectric transition. The other curve represents the temperature dependence of spontaneous polarization as calculated from Eq. (10).

The pyroelectric characteristic was employed to assess the polarization state of samples previously poled at different conditions of electric field and time. Samples poled at RT and 80 °C were subjected to heating at a constant rate and the pyrocurrent was monitored for both (Fig. 9). It is clear that the sample poled at RT (no hump in the poling current curve) has very low pyroelectric activity while the sample poled at 80 °C showed a significantly higher pyroelectric activity. The same procedure was repeated for different samples previously poled at the same electric field (4 kV/cm) at RT for 10 and 250 s (Fig. 10). For 10 s poling the current did not hump since the time was too short. For 250 s the hump was observed as expected. The pyrocurrent measured for the non-humping poling curve showed a much lower pyroelectric coefficient than the humping curve (Fig. 11). It should be noted that a further increase of the temperature during poling leads to rapid depolarization due to the pyroelectric effect, as will be elaborated elsewhere.<sup>32</sup>

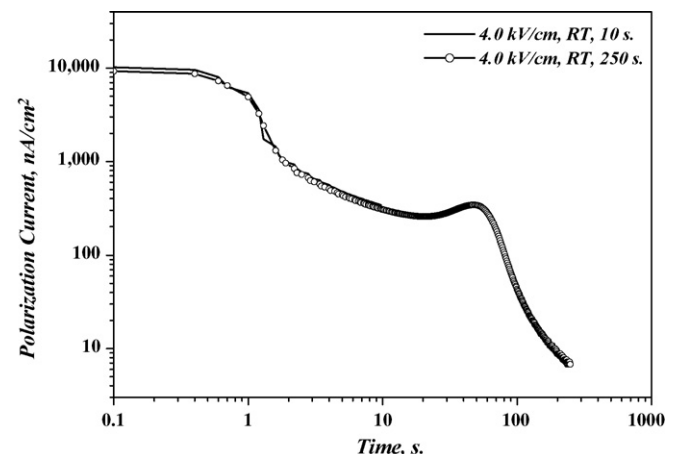


Fig. 10. Poling current of two samples poled at 4.0 kV/cm at room temperature for different poling time.

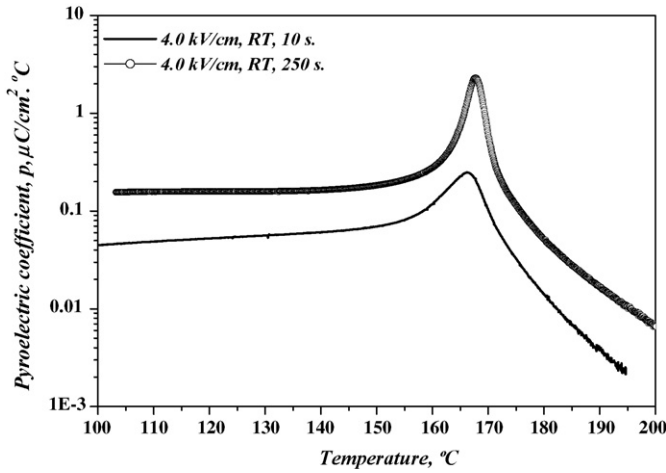


Fig. 11. Pyroelectric coefficient of the two samples poled as shown in Fig. 12.

As a final confirmation of the significance of the appearance of the hump in the poling curve as finger-print of the full polarization the following test has been carried out. Two samples were poled at 3.75 and 4.75 kV/cm for  $10^3$  s at RT. They both showed a humped poling curve (Fig. 13). The pyrocurrent was measured for both and it was found that for both samples the pyroelectric coefficient peaks were almost identical (Fig. 13).

Fig. 14 shows a significant increase of residual polarization by increasing the poling field. The remanent polarization as observed by hysteresis loop versus temperature measurements shows a higher magnitude than that of the calculated polarization from pyroelectricity. This difference can be attributed to the back-switching of some reversible domains after removing the field.<sup>11</sup>

4.5. Dielectric properties

Fig. 15 shows the temperature dependence of the relative permittivity at 1 kHz for different samples poled at different poling fields including a non-poled sample. The relative permittivity typically drastically increases as the temperature increases

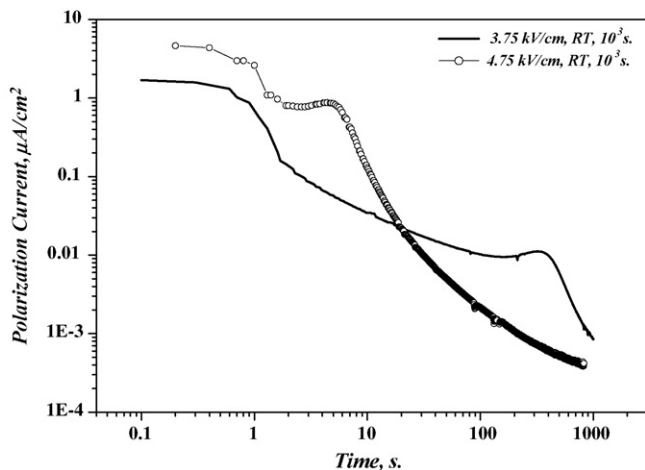


Fig. 12. Poling current of two samples poled at 3.75 and 4.75 kV/cm at room temperature for  $10^3$  s.

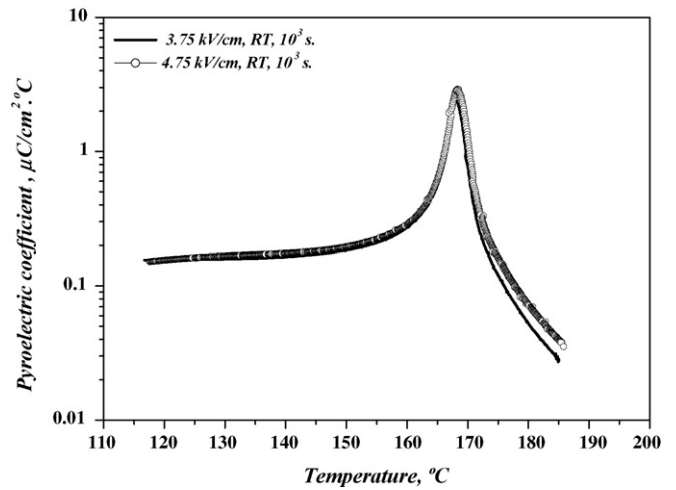


Fig. 13. Pyroelectric coefficient of the two samples poled as shown in Fig. 14.

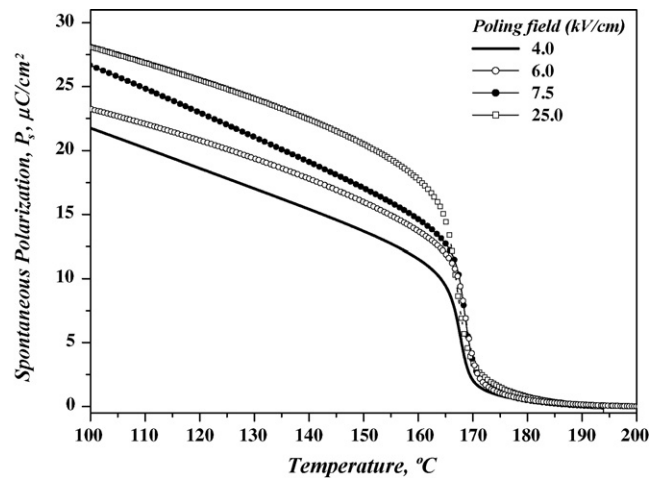


Fig. 14. Spontaneous polarization as a function of temperature (after poling with different electric fields) as calculated from pyroelectric coefficient.

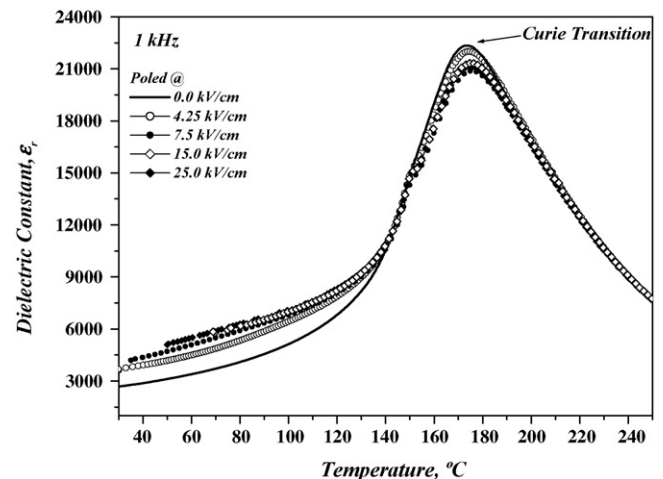


Fig. 15. Relative permittivity as a function of temperature at 1 kHz after poling with different poling electric fields.

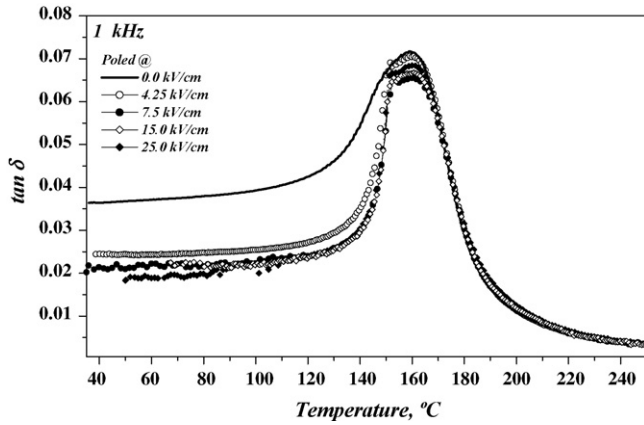


Fig. 16. Dielectric loss factor as a function of temperature at 1 kHz after poling with different poling electric fields.

Table 1

PXE52 properties

Density ( $\text{g}/\text{cm}^3$ )	7.45
Grain size ( $\mu\text{m}$ )	4.5
Curie temperature ( $^{\circ}\text{C}$ )	168 ( $I_{\text{pyro}}-T$ ); 170 ( $P_r-T$ ); 175 ( $\epsilon_r-T$ )
Resistivity, $\rho$ ( $\Omega\text{ cm}$ )	$3.4 \times 10^{10}$
Relative permittivity (1 kHz/RT)	2260 (non-poled); 5160 (after 25 kV/cm)
$\tan \delta$ (1 kHz/RT)	0.036 (non-poled); 0.018 (after 25 kV/cm)
Maxwell–Wagner time constant, $\tau = RC$ (s)	$\sim 2.58$
Remanent polarization, $P_r$ ( $\mu\text{C}/\text{cm}^2$ )	35.7
Saturation polarization, $P_{\text{sat}}$ ( $\mu\text{C}/\text{cm}^2$ )	42.5
Coercive field, $E_C$ (kV/cm)	7.47
Pyroelectric coefficient, $p$ at $T_C$ ( $\mu\text{C}/(\text{m}^2\ ^{\circ}\text{C})$ )	$4.8 \times 10^{-4}$

to peak at 175  $^{\circ}\text{C}$  and thereafter decreases again. In the low-temperature region (in the ferroelectric phase) the poling field (until 7.5 kV/cm) shows significant enhancement of the relative permittivity and no further enhancement is noticed for poling fields higher than 7.5 kV/cm.

As the poling field enhances the relative permittivity near room temperature it suppresses the peak height at the Curie transition and has no influence in the paraelectric phase. Fig. 16 shows the dielectric loss factor as a function of temperature. The poling field considerably reduces the loss factor till 7.5 kV/cm while no further effect was noticed at higher fields. As a common behavior in polycrystalline ferroelectric material the loss factors peaks at a temperature lower than the Curie transition temperature.<sup>21</sup> For convenience, Table 1 summarizes the physical properties for PXE52.

## 5. Discussion

### 5.1. Interpretation of the polarization current curves

As has been shown in the hysteresis loop measurements, the coercive field is about 7.5 kV/cm. The polarization current curves (Fig. 4) revealed that the threshold field needed to view the hump within 500 s at room temperature is  $\sim (1/2)E_C$ . Keep

in mind that the coercive field is not an absolute quantity<sup>12</sup> since by subjecting a non-poled sample to a low field for long time interval the polarization will eventually switch. In other words, since for a virgin sample (not poled) there is no net polarization, on average the positive polarization  $(+1/2)P$  and the negative polarization  $(-1/2)P$  cancel and the field necessary to switch one to the other, or at least to make a net (non-zero) dipole moment, is approximately  $(1/2)E_C$ , as is experimentally observed.

The polarization of PZT is provided by 180 $^{\circ}$  and/or 90 $^{\circ}$  (for tetragonal structure) and 71 $^{\circ}$  and/or 109 $^{\circ}$  (for rhombohedral structure). All types of switching can occur, however, the distinction between the different types cannot be made without further information.

The polarization current curves (Figs. 4 and 7) for low and high fields, respectively, can be divided into three regions:

- Region I: Maxwell–Wagner polarization,<sup>25–29</sup>
- Region II: polarization switching<sup>11–18</sup> and
- Region III: steady-state conduction current.<sup>10</sup>

We assume that the low-field curves (Fig. 4) show only regions I and II since, as we said earlier, at low fields a steady-state current was not reached. On the other hand, the high-field curves (Fig. 7) show only a tail of regions II and III. In the following, we discuss in some detail the mechanism occurring in each region at low and high poling electric fields.

### 5.2. Low-field regime

Applying a poling dc field to a ferroelectric ceramic leads to so-called Maxwell–Wagner polarization<sup>25–29</sup> indicated by an initial current which is decaying by time constant  $\tau = R_B C_{GB}$ , where, according to Waser,<sup>25–28</sup>  $R_B$  is the grain bulk resistance and  $C_{GB}$  is the grain boundary capacitance. The current decays as

$$J_{\text{MW}} = J_0 e^{-t/\tau}$$

The Maxwell–Wagner (M–W) (or space charge polarization as it is referred to in some texts<sup>28</sup>) is limited to short time only (region I). The space charge polarization is attributed to the pile up and depletion of the mobile charge carriers that arise at the interface between two different media,<sup>25–28,30</sup> leading to a limited transport until the charge carriers are stopped at a potential barrier, possibly a grain boundary.<sup>2</sup> The resultant current due to this polarization decays until the charging of the barrier capacitor is completed.<sup>28</sup> For that reason, M–W or space charge polarization is limited to short time only. The polarization current curves in Fig. 4 show initial current decays with a time constant ( $\tau \sim 2.6$  s) for all fields.

Maxwell–Wagner polarization is followed by polarization switching (region II), characterized by a limited window of applied fields  $((1/2)E_C - E_C)$  for which the polarization current shows a hump due to the switching of the antiparallel dipoles ( $-P \rightarrow +P$ ).<sup>13,14</sup> As stated by Merz<sup>13</sup> and Merz and Fatuzzo<sup>14</sup> and many others,<sup>11,12,15,16</sup> the switching process shows that, the higher the applied field, the faster the appearance of the

hump, implying a faster dipole switch and thus a larger peak current  $J_{\max}$ . As shown in Figs. 5 and 6, at higher temperature the switching time becomes shorter and thus the switching current increases significantly.<sup>13</sup>

For extremely low field or moderate field applied for shorter time, the hump is not observed, Figs. 5 and 10. That means that switching is not complete. In other words, the polarization did not reach its full magnitude, as confirmed by the pyroelectric current curves, Figs. 9 and 11.

The total switching polarization is given by Eq. (7). Due to its extremely fast response and negligible magnitude compared to the second term, the first term is negligible.<sup>12,14,15,18</sup> For non-poled material there is no initial polarization and the total area under the poling current curve gives  $P$  instead of  $2P$ . Consequently, Eq. (7) becomes:

$$\int_0^{\infty} J(t) dt = P \quad (11)$$

Since the current decreases exponentially, the total switching time  $t_{\text{sw}}$  is usually taken as the value where current falls to  $0.1J_{\max}$ .<sup>12</sup>

Since switching occurs at any field given enough time, the polarization is independent of the field and the charge density is constant after the switching time.<sup>15</sup> Therefore, Eq. (11) becomes

$$\int_0^{t_{\text{sw}}} J(t) dt = P_{\text{sw}} = \text{constant} \quad (12)$$

This can be verified by examining Figs. 11 and 12. When different fields are applied on two samples, given long enough time for the current to reach  $0.1J_{\max}$ , the two samples show equal pyroelectric activity. Table 2 shows the switching polarization for different poling fields and shows that the charge density is indeed constant.

Worthwhile to mention is that, it is believed that there is no ionic polarization in polar dielectrics, since the permanent dipoles already exist in the material. Polar materials reveal a tendency towards dipolar or rotational polarization.<sup>33</sup> Dipolar polarization is characterized by a slow behavior<sup>33</sup> as can be observed from the polarization current curves. Adding to that, the ionic polarization requires a time as short as  $\sim 10^{-12}$  s<sup>33</sup> and therefore is impossible to be detected by our experiment. This implies that this process is already beyond the time scale discussed in the paper.

Table 2  
Polarization results according to Merz's theory

Applied poling field (kV/cm)	$J_{\max}$ (nA/cm <sup>2</sup> )	Switching time, $t_s$ (s)	Switching polarization, $P_{\text{sw}}$ ( $\mu\text{C}/\text{cm}^2$ ) (according to Eq. (12))
3.75	63.08	590	26
4.0	196.9	213	26.7
4.25	564	71	26.7
4.5	2,480	15.6	24.5
4.75	3,952	9.8	24.9
5.0	11,119	3.3	26.3

### 5.3. High-field regime

At high field the domain growth is extremely rapid.<sup>13</sup> By means of our techniques it is not possible to record the maximum polarization current (the hump) and the corresponding switching time. For that reason, the higher the applied field, the lower the initial current. In other words, at high field we see only the decaying tail of the hump at the very beginning of the experimental curve. If we integrate the experimental  $J-t$  curve to calculate the polarization, the charge will be lower than that for the low-field case since the integration range is incomplete. In reality this is not the case. Calculating the spontaneous polarization from pyroelectricity we found the higher the applied field, the higher the polarization (Fig. 14), as expected.

Contrary to the low-field regime, the current at high electric field shows a steady state at very long time. This steady state increases with increasing applied field in such a way that the ratio  $E/J$  gives a constant value. The steady-state current is ascribed to electrical conduction of the material<sup>10</sup> and the constant ratio  $E/J$  represents the electrical resistivity  $\rho$  (Table 1).

In a recent paper Lubascu et al.<sup>34</sup> showed also the time dependence of the polarization process when reversing the direction of the electric field, but only at high fields. The fast response is attributed to domain switching only. Our results corroborate theirs since in our  $E < E_C$  polarization results, only the tail of M–W process can be identified. For the  $E > E_C$  polarization current decreases with increasing the electric field and refers to the domain switching only. The long time scale tail is attributed to the steady-state conduction current.

## 6. Conclusions

Poling is a crucial step in the manufacturing process for ferroelectric materials and in this paper the poling state has been determined phenomenologically by different techniques. It appears that the pyroelectric activity, regardless its own usage, can be used as a good tool to measure the degree of polarization. The polarization current in the low-field regime can be described with the switching polarization theory and according to this theory, for optimal poling, an electric field slightly higher than  $E_C$  field should be applied at least for the switching time of the domains at room temperature. Contrary to common practice, good dielectric and ferroelectric properties can be reached at room temperature at a field slightly larger than the coercive field. Finally, the material showed high stable electrical insulation and no resistance degradation has been observed.

## Acknowledgements

The authors would like to express their great thanks to Dr. W.A. Groen and Mr. K. Prijs (*Morgan Electro Ceramics*, BV Eindhoven, the Netherlands) for providing the samples and other technical help. T.M. Kamel is very grateful to Dr. B. Noheda (Groningen University, Groningen, the Netherlands) for her fine and kind cooperation. Financial support for this work, carried out in the framework of the research program TS, by SENTER is greatly appreciated.



## References

1. Jaffe, B., Cook, W. R. and Jaffe, H., *Piezoelectric Ceramics*. Academic Press, New York, 1971.
2. Moulson, A. J. and Herbert, J. M., *Electroceramics*. Chapman & Hall, London, 1991.
3. Setter, N., *Piezoelectric Materials in Devices*. Ceramics Laboratory, EPFL, 2003.
4. Ravez, J., *C. R. Acad. Sci. Paris Ser. IIC, Chim./Chem.*, 2000, **3**, 267.
5. Sayer, M., Judd, B. A., El Assal, K. and Prasad, E., *J. Can. Ceram. Soc.*, 1981, **50**.
6. Kholkin, L., Taylor, D. V. and Setter, N., *ISAF-XI*, August 24–27, 1998, p. 69.
7. Wang, H.-W., Cheng, S.-Y. and Wang, C.-M., In *IEEE/CHMT Japan IEMT Symposium*, 1989, p. 263.
8. Raibagkar, L. J. and Bajaj, S. B., *Solid State Ionics*, 1998, **108**, 105.
9. Kim, S.-B., Kim, D.-Y., Kim, J.-J. and Cho, S.-H., *J. Am. Ceram. Soc.*, 1990, **73**, 161.
10. Jonscher, A. K., *Dielectric Relaxation in Solids*. Chelsea Dielectrics, London, 1983.
11. Damjanovic, D., *Rep. Prog. Phys.*, 1998, **61**, 1267.
12. Burfoot, J. C. and Taylor, G. W., *Polar Dielectrics and their Applications*. University of California Press, Berkeley and Los Angeles, 1979.
13. Merz, W. J., *Phys. Rev.*, 1954, **95**, 690.
14. Fatuzzo, E. and Merz, W. J., *Phys. Rev.*, 1959, **116**, 61.
15. Pulvari, C. F. and Keubler, W., *J. Appl. Phys.*, 1958, **29**, 1315.
16. Böttger, U., In *Polar Oxides*, ed. R. Waser, U. Böttger and S. Tiedke. Wiley-VCH Verlag GmbH & Co. KGaA, Weinheim, 2005, and references therein.
17. Drougard, M. E., *J. Appl. Phys.*, 1960, **31**, 352.
18. White, P. H. and Withey, B. R., *Br. J. Appl. Phys.*, 1969, **2**, 1487.
19. Hammer, M. and Hoffmann, M. J., *J. Am. Ceram. Soc.*, 1998, **81**, 3277.
20. Lang, S. B., *Source Book of Pyroelectricity*. Gordon and Breach Science Publishers, London, 1974.
21. Lines, M. E. and Glass, A. M., *Principles and Applications of Ferroelectrics and Related Materials*. Clarendon Press, Oxford, 1977.
22. Safari, A., Panda, R. K. and Janas, V. F., *Key Eng. Mater.*, 1996, **35**, 122.
23. Elissalde, C. and Ravez, J., *J. Mater. Chem.*, 2001, **11**, 1957.
24. Pan, W. Y., Shroud, T. R. and Cross, L. E., *J. Mater. Sci. Lett.*, 1989, **8**, 771.
25. Vollman, M. and Waser, R., *J. Am. Ceram. Soc.*, 1994, **77**, 235.
26. Waser, R. and Hagenbeck, R., *Acta Mater.*, 2000, **48**, 797.
27. Vollman, M. and Waser, R., *J. Electroceram.*, 1997, **1**, 51.
28. Hölbling, T. H., Söylemezoğlu, N. and Waser, R., *J. Electroceram.*, 2002, **9**, 87.
29. Bouyssou, E., Leduc, P., Guégan, G. and Jérésian, R., *J. Phys.*, 2005, **10**, 317.
30. Hill, N. E., Vaughan, W. E., Price, A. H. and Davies, M., *Dielectric Properties and Molecular Behaviour*. Van Nostrand, Reinhold, London, 1969.
31. Strukov, B. A. and Levanyuk, A. P., *Ferroelectric Phenomena in Crystals*. Springer-Verlag, Berlin, Heidelberg, 1998.
32. Kamel, T. M. and de With, G., in press.
33. Tareev, B., *Physics of Dielectric Materials*. Mir Publishers, Moscow, 1975.
34. Lupascu, D. C., Fedosov, S., Verdier, C., Rödel, J. and von Seggern, H., *J. Appl. Phys.*, 2004, **95**, 1386.